Detection of Gravitational Wave Event GW170817 is First with Electromagnetic Signature

---from a Binary Neutron Star Merger detected by the Laser Interferometric Gravitational Wave Observatory (LIGO)

by
Bill Gabella

26 June 2018

References: http://ligo.org/ Ligo website, and GW170817 LIGO Page
Physical Review Letters detection paper
Astrophysical Journal Letters, Focus on EM Counterpart
Ligo page with video and graphic here

“Seen” by Hanford, Livingston, and VIRGO

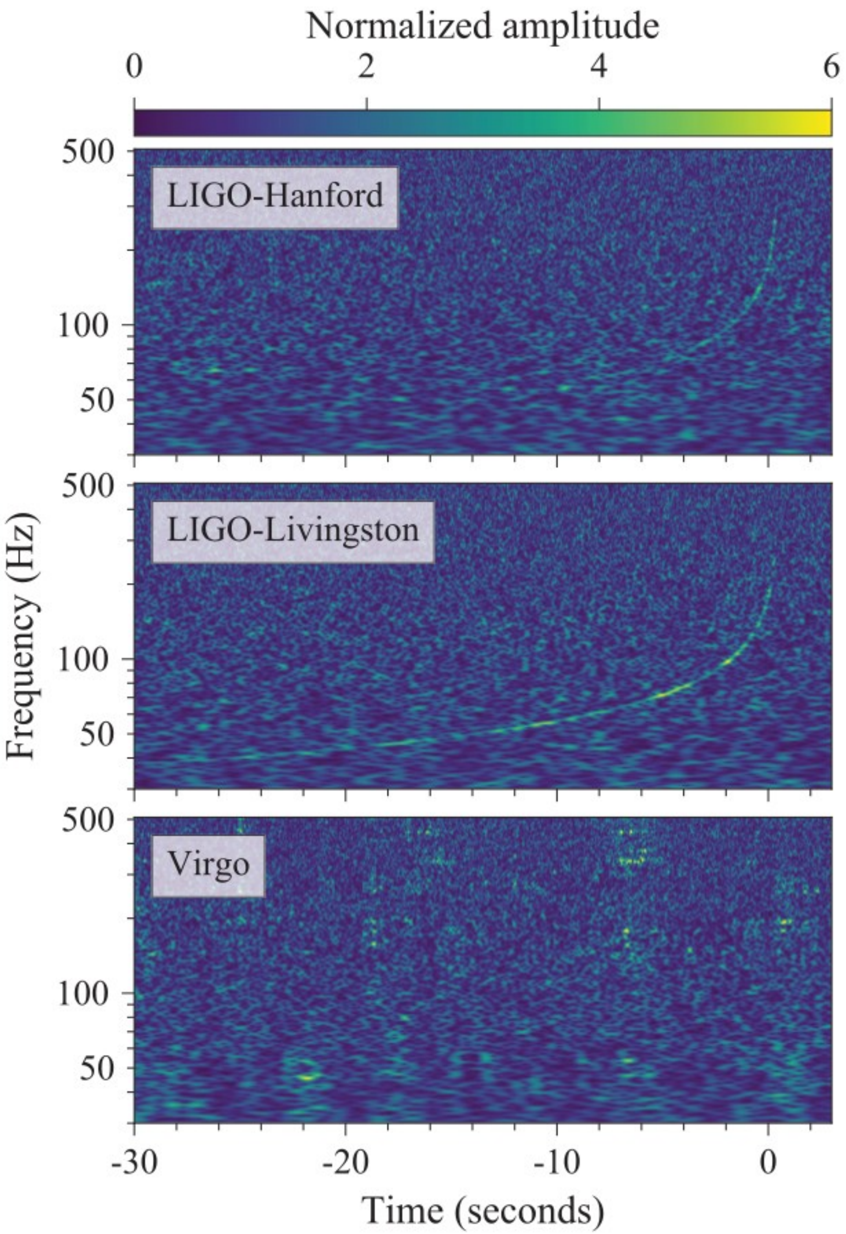

FIG. 1. Time-frequency representations [65] of data containing the gravitational-wave event GW170817, observed by the LIGO-Hanford (top), LIGO-Livingston (middle), and Virgo (bottom) detectors. Times are shown relative to August 17, 2017 12:41:04 UTC. The amplitude scale in each detector is normalized to that detector’s noise amplitude spectral density. In the LIGO data, independently observable noise sources and a glitch that occurred in the LIGO-Livingston detector have been subtracted, as described in the text. This noise mitigation is the same as that used for the results presented in Sec. IV.

"Glitch" in the Livingston LIGO Data Stream

- Kept LO from sending out an automated message to the collaboration and other astronomers.

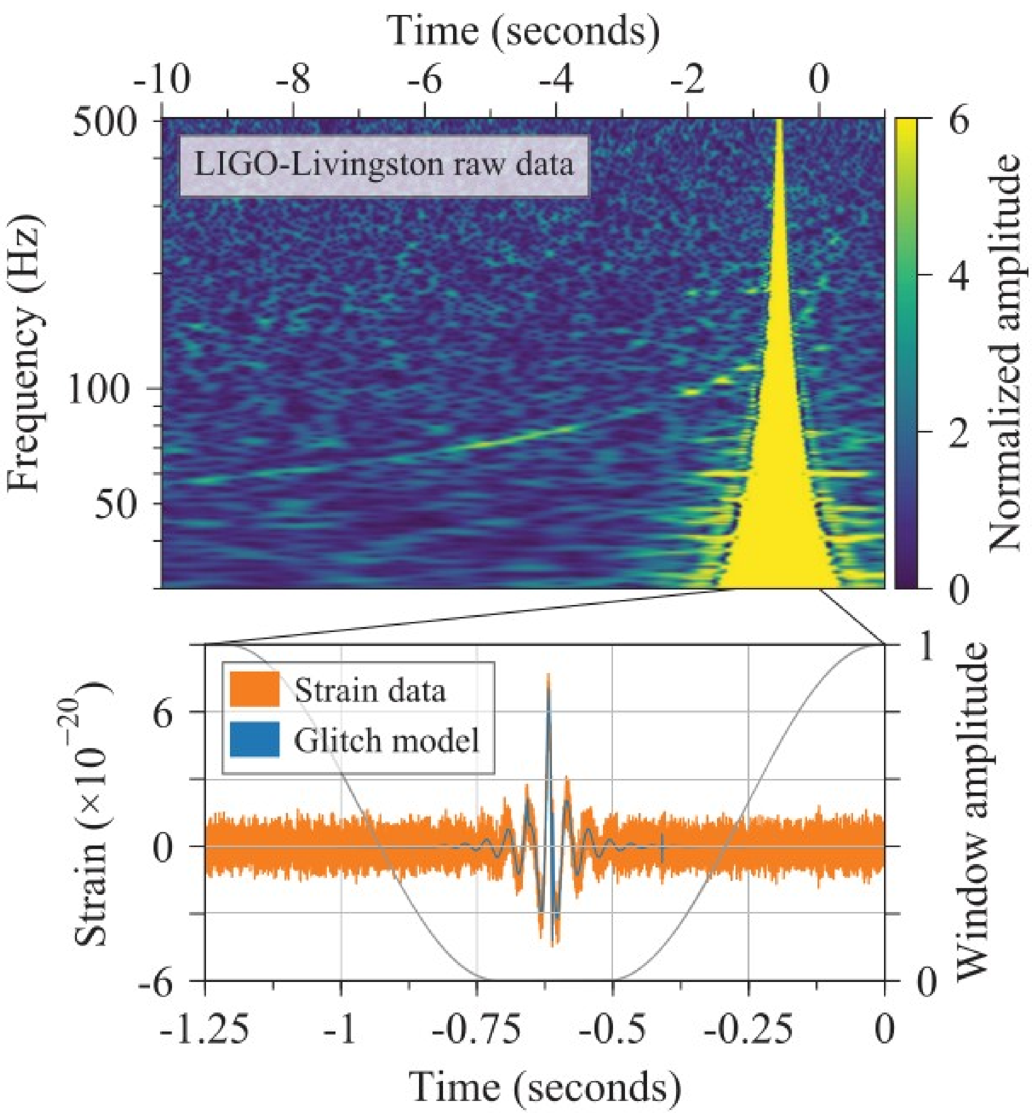

FIG. 2. Mitigation of the glitch in LIGO-Livingston data. Times are shown relative to August 17, 2017 12:41:04 UTC. *Top panel*: A time-frequency representation [65] of the raw LIGO-Livingston data used in the initial identification of GW170817 [76]. The coalescence time reported by the search is at time 0.4 s in this figure and the glitch occurs 1.1 s before this time. The time-frequency track of GW170817 is clearly visible despite the presence of the glitch. *Bottom panel*: The raw LIGO-Livingston strain data (orange curve) showing the glitch in the time domain. To mitigate the glitch in the rapid reanalysis that produced the sky map shown in Fig. 3 [77], the raw detector data were multiplied by an inverse Tukey window (gray curve, right axis) that zeroed out the data around the glitch [73]. To mitigate the glitch in the measurement of the source's properties, a model of the glitch based on a wavelet reconstruction [75] (blue curve) was subtracted from the data. The time-series data visualized in this figure have been bandpassed between 30 Hz and 2 kHz so that the detector's sensitive band is emphasized. The gravitational-wave strain amplitude of GW170817 is of the order of 10^{-22} and so is not visible in the bottom panel.

GW170817 Properties

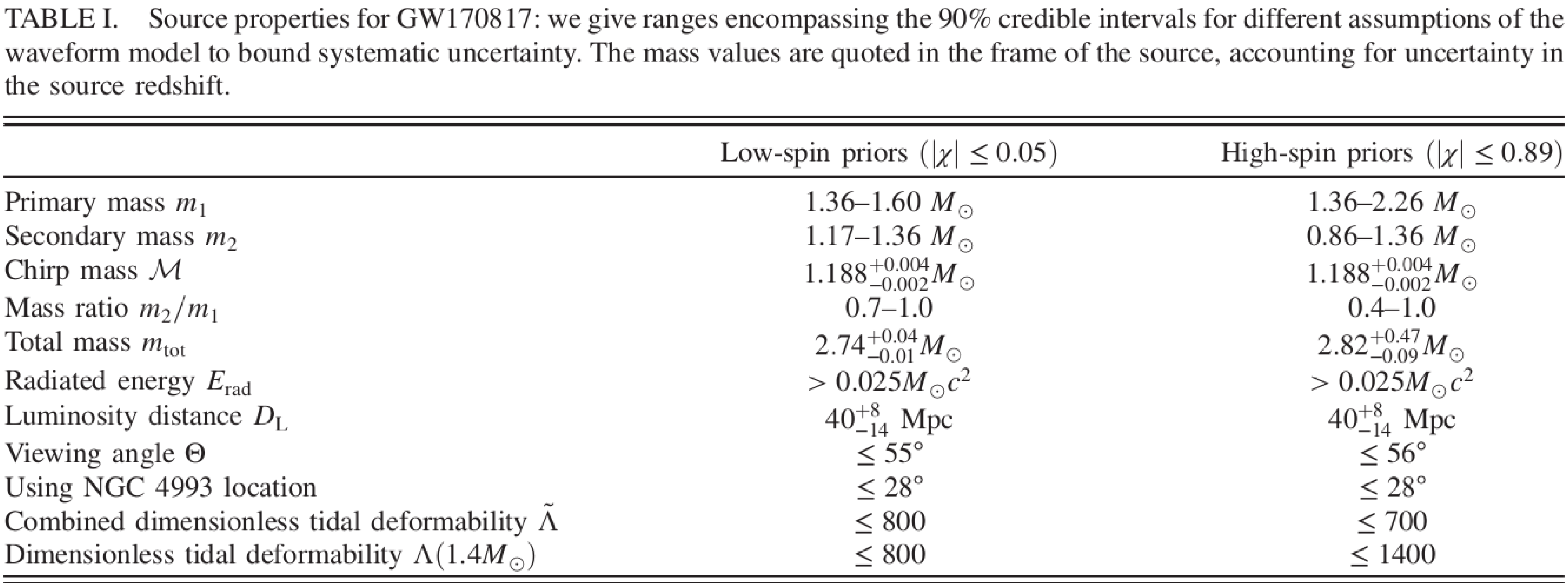

TABLE I. Source properties for GW170817: we give ranges encompassing the 90% credible intervals for different assumptions of the waveform model to bound systematic uncertainty. The mass values are quoted in the frame of the source, accounting for uncertainty in the source redshift.

	Low-spin priors ($\lvert\chi\rvert \leq 0.05$)	High-spin priors ($\lvert\chi\rvert \leq 0.89$)
Primary mass m_1	1.36–1.60 $M_\odot$	1.36–2.26 $M_\odot$
Secondary mass m_2	1.17–1.36 $M_\odot$	0.86–1.36 $M_\odot$
Chirp mass $\mathcal{M}$	$1.188^{+0.004}_{-0.002} M_\odot$	$1.188^{+0.004}_{-0.002} M_\odot$
Mass ratio m_2/m_1	0.7–1.0	0.4–1.0
Total mass m_{tot}	$2.74^{+0.04}_{-0.01} M_\odot$	$2.82^{+0.47}_{-0.09} M_\odot$
Radiated energy E_{rad}	$> 0.025 M_\odot c^2$	$> 0.025 M_\odot c^2$
Luminosity distance D_{L}	40^{+8}_{-14} Mpc	40^{+8}_{-14} Mpc
Viewing angle Θ	$\leq 55°$	$\leq 56°$
Using NGC 4993 location	$\leq 28°$	$\leq 28°$
Combined dimensionless tidal deformability $\tilde{\Lambda}$	≤ 800	≤ 700
Dimensionless tidal deformability $\Lambda(1.4 M_\odot)$	≤ 800	≤ 1400

Low spins most likely (though like msec pulsars some think they can spin up), <= 0.05, so call it a m_1 of 1.48 Msol and m_2 of 1.27 Msol.
GWs estimate Distance 40 Mpc BUT +8 and -14 Mpc error bars!
Galaxy NGC 4993 is 40 Mpc away.

Cosmological Distances, parsec (pc) and light-year (ly)

Milky Way Diameter 100 k ly (smallish for a galaxy)
Large Magellanic Cloud distance 158k ly
Andromeda Galaxy distance 2.54M ly 0.78 Mpc
Local Group (of 54 galaxies) diameter 10M ly   3.1 Mpc

NGC 4993   130 Mly   40 Mpc

Most distant object GN-z11 13.4 Gly 4.1 Gpc   z=11.1

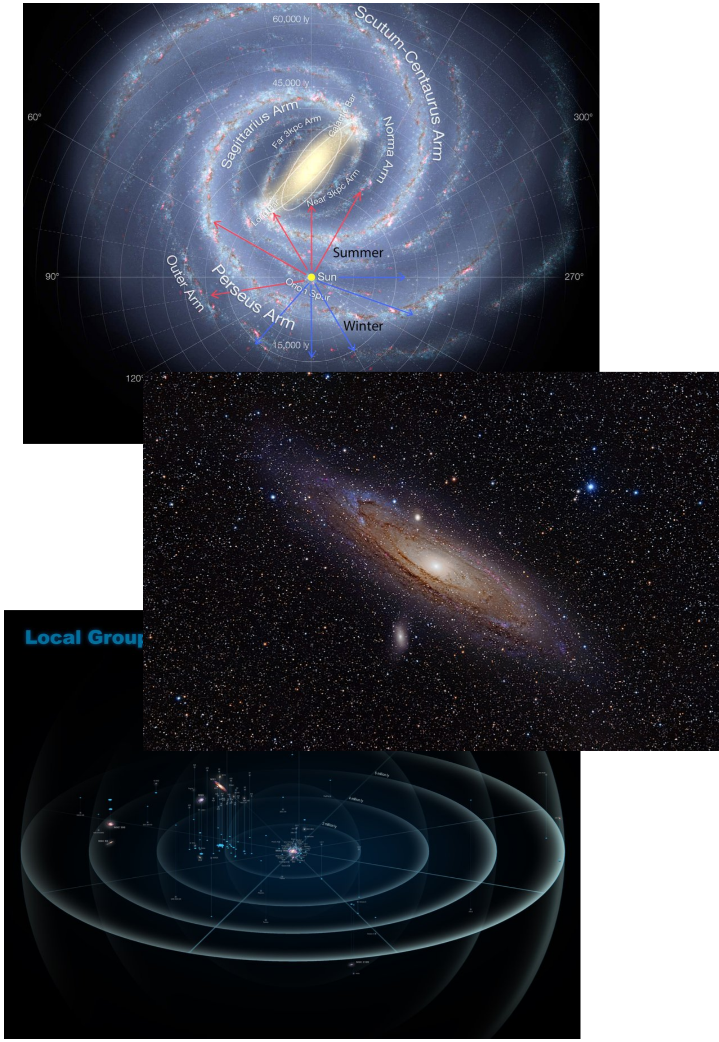

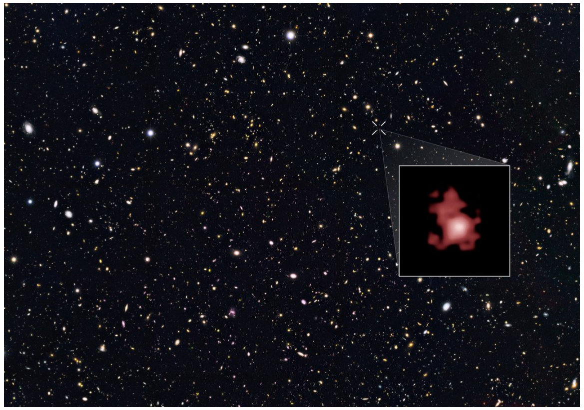

1 au	1.496e11 m	earth-sun distance on average
1 ly	9.4607e15 m	
1 pc	3.086e16 m	3.262 ly

Sky Location from LIGO-VIRGO detector "constellation"

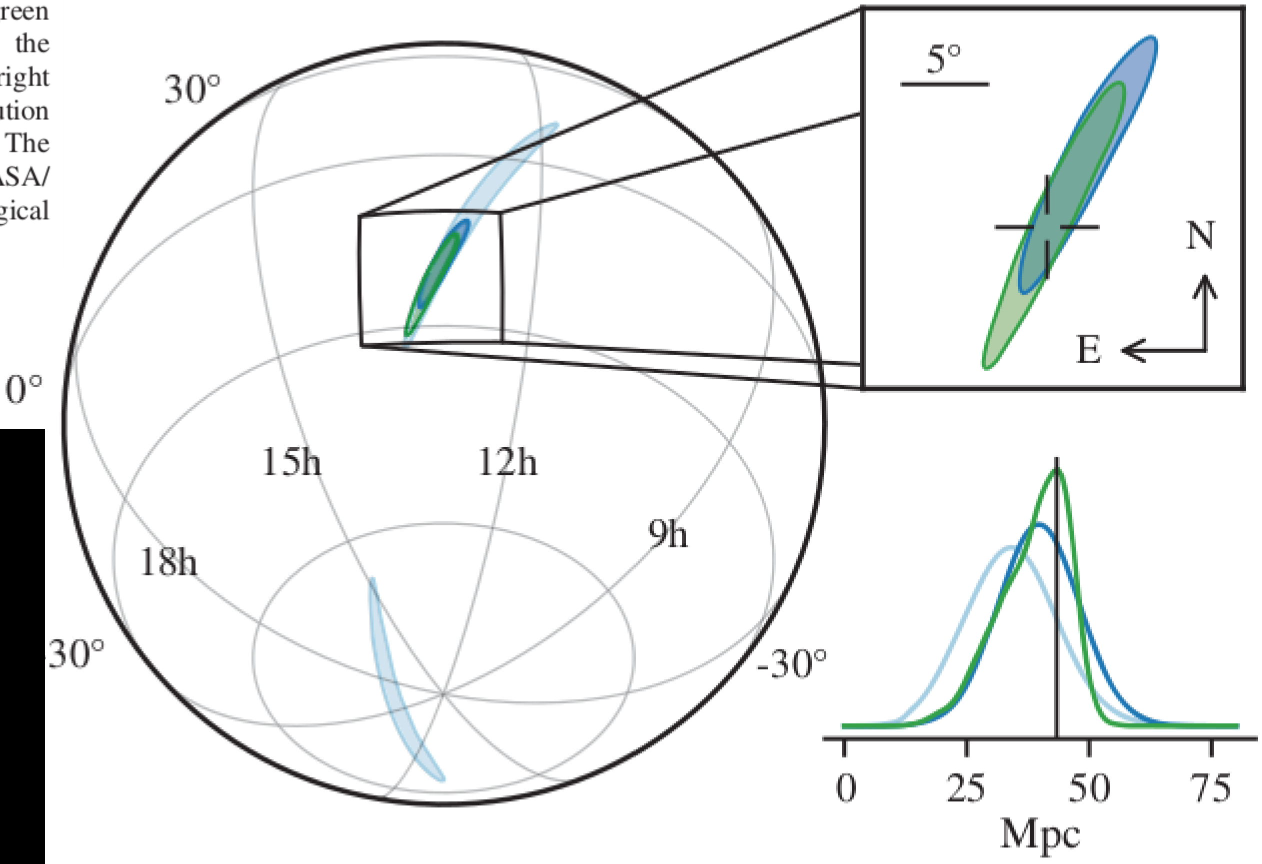

FIG. 3. Sky location reconstructed for GW170817 by a rapid localization algorithm from a Hanford-Livingston (190 deg^2, light blue contours) and Hanford-Livingston-Virgo (31 deg^2, dark blue contours) analysis. A higher latency Hanford-Livingston-Virgo analysis improved the localization (28 deg^2, green contours). In the top-right inset panel, the reticle marks the position of the apparent host galaxy NGC 4993. The bottom-right panel shows the *a posteriori* luminosity distance distribution from the three gravitational-wave localization analyses. The distance of NGC 4993, assuming the redshift from the NASA/IPAC Extragalactic Database [89] and standard cosmological parameters [90], is shown with a vertical line.

Other Sky Localizations

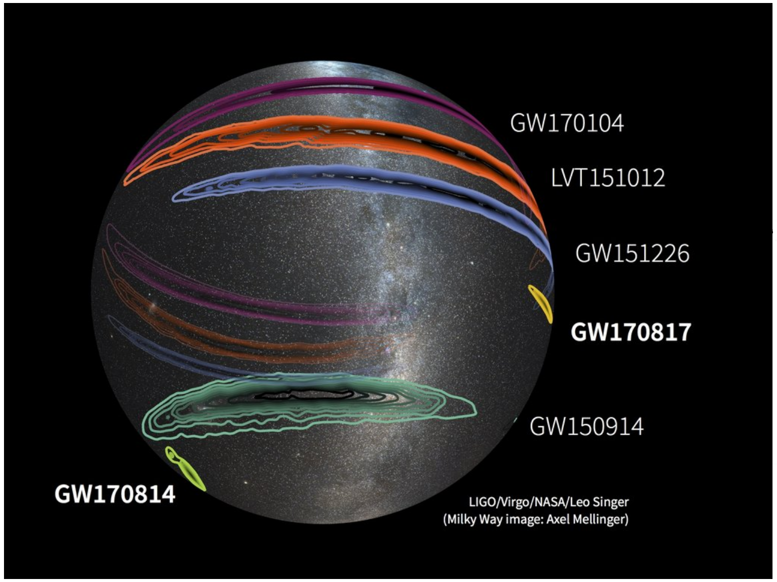

LIGO/Virgo/NASA/Leo Singer
(Milky Way image: Axel Mellinger)

Telescopes found the corresponding "kilonova" in galaxy NGC 4993

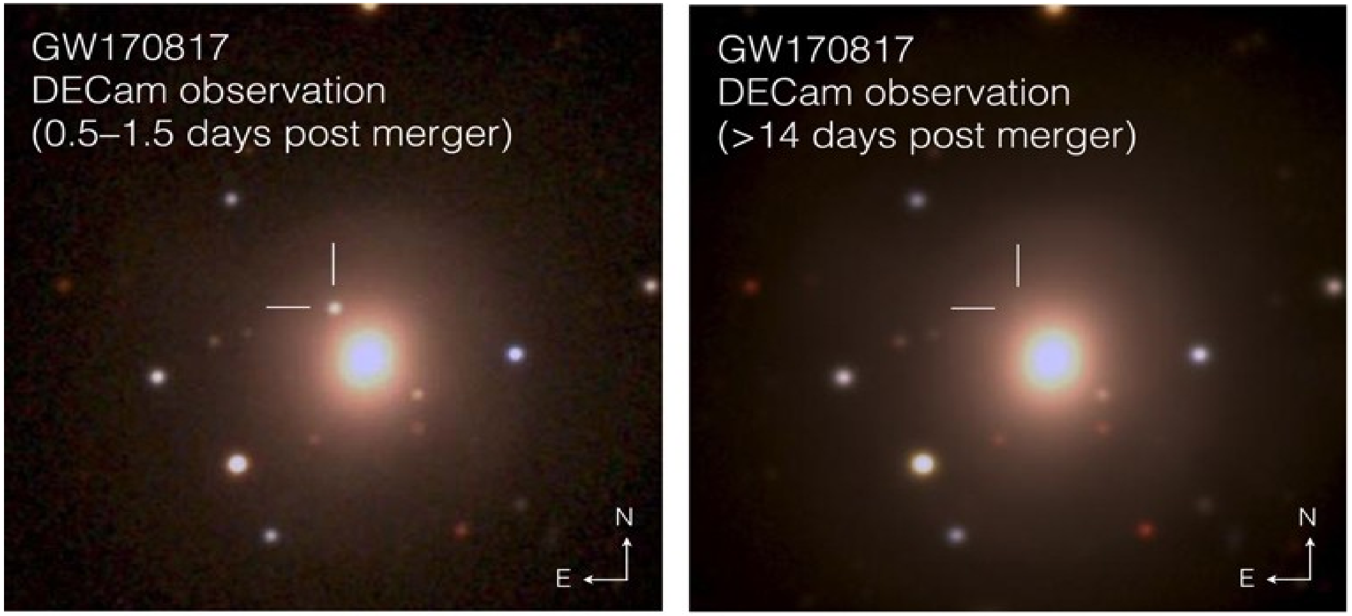

Figure 1 from The Electromagnetic Counterpart of the Binary Neutron Star Merger LIGO/Virgo GW170817. I. Discovery of the Optical Counterpart Using the Dark Energy Camera
M. Soares-Santos et al. 2017 ApJL 848 L16 doi:10.3847/2041-8213/aa9059
http://iopscience.iop.org/article/10.3847/2041-8213/aa9059/meta

GW170817 on YouTube

Max-Planck-Insitut simulation, 46s   Simulation video

NCSA Numerical Relativity, 2m8s   BNS Simulation

Flashy Video from Ligo-Virgo, 4m17s   Description of event
... and at 3m23s artistic merger   merger with explosion

Zoom in on Kilonova NGC4993   here

Population of Black Holes and Neutron Stars

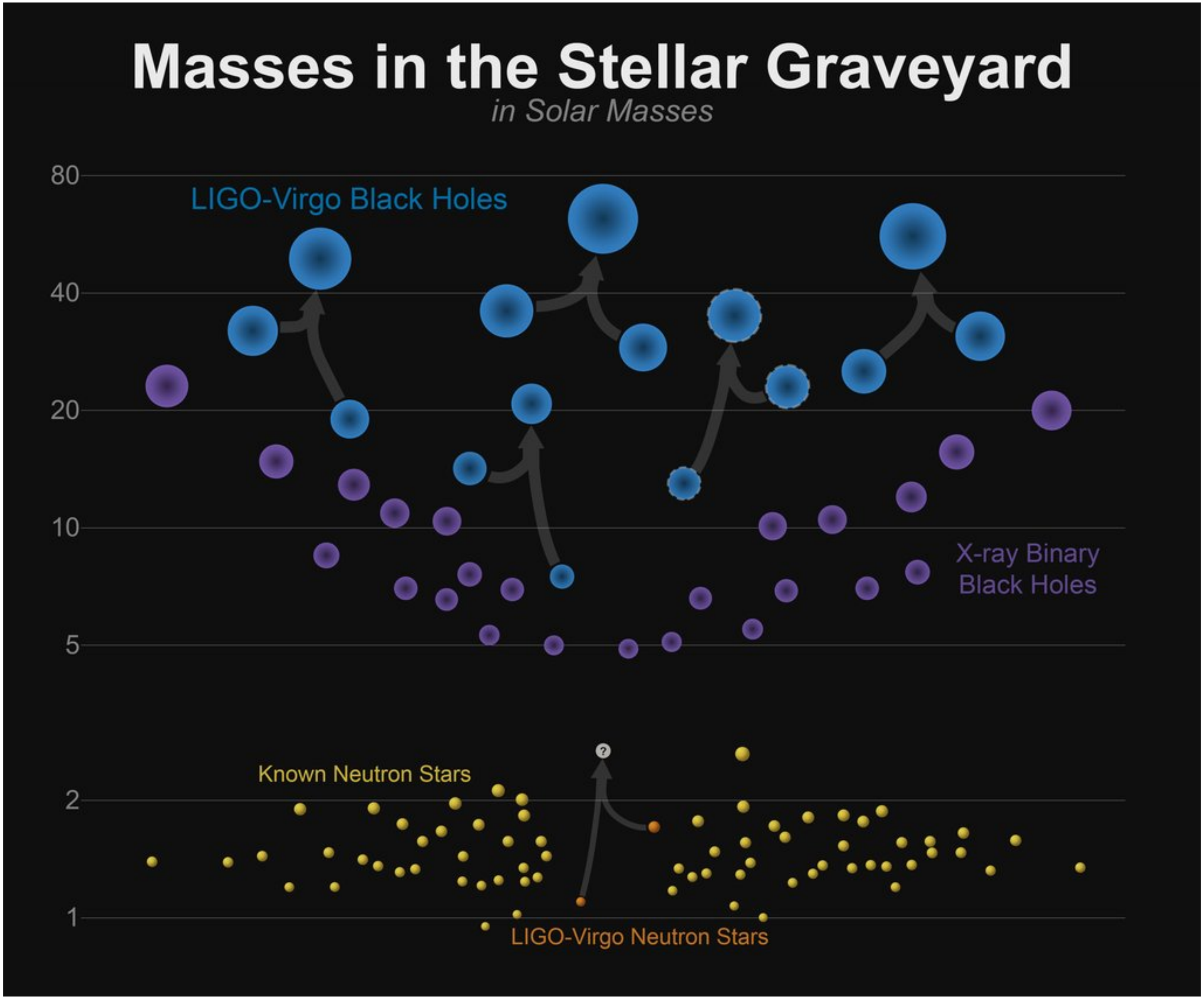

GW170817 with other BH GW Sources

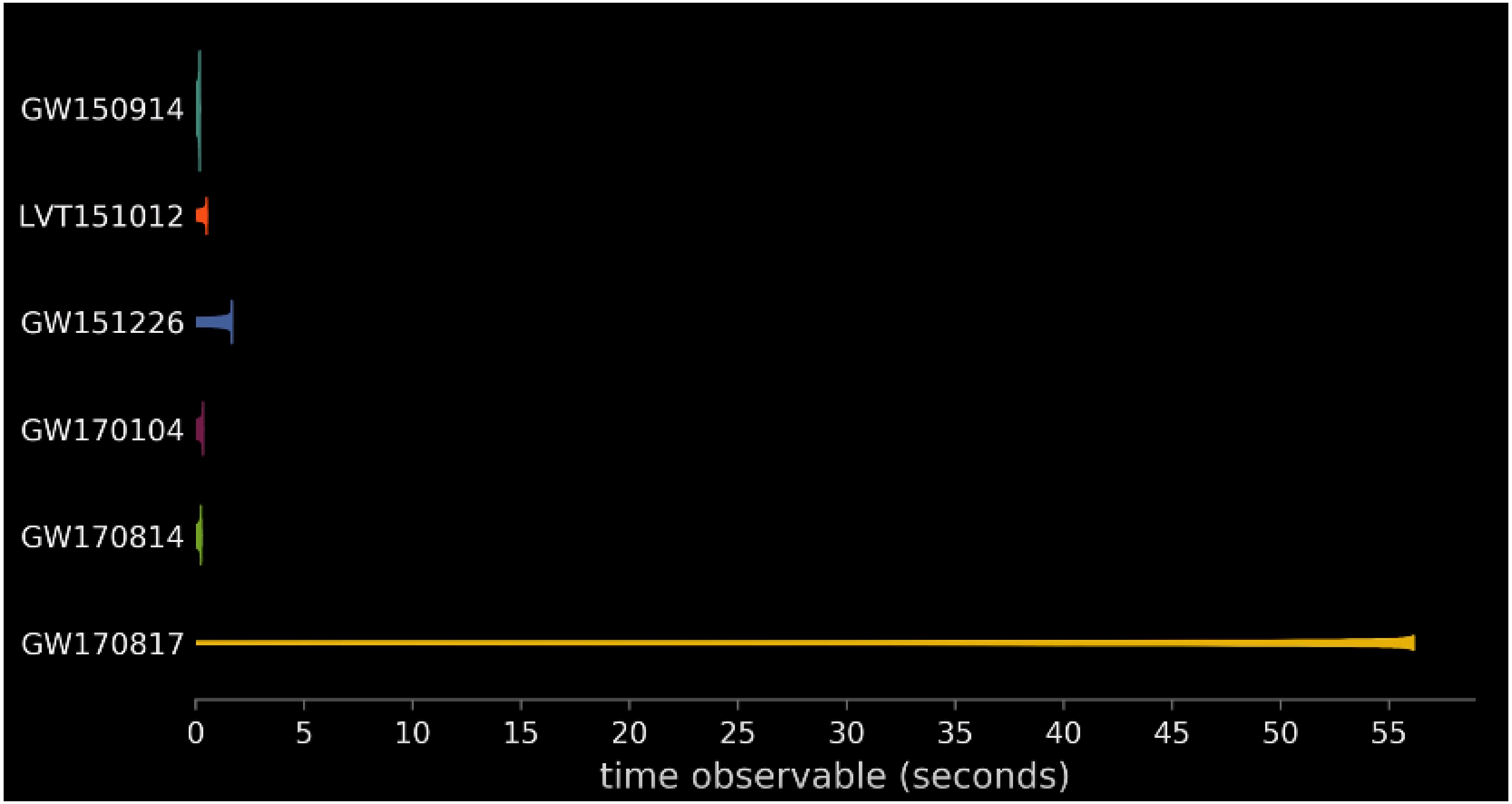

YouTube video here

GW170817 Observed in all electromagnetic bands: Gamma rays, x-rays, UV, Visible, IR, and Radio

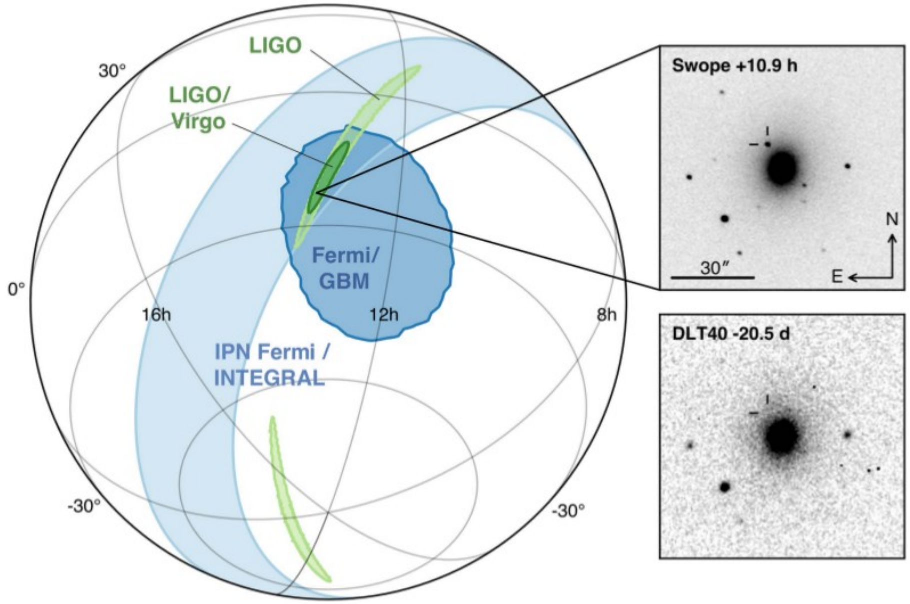

Figure 1. Localization of the gravitational-wave, gamma-ray, and optical signals. The left panel shows an orthographic projection of the 90% credible regions from LIGO (190 deg^2; light green), the initial LIGO-Virgo localization (31 deg^2; dark green), IPN triangulation from the time delay between *Fermi* and *INTEGRAL* (light blue), and *Fermi*-GBM (dark blue). The inset shows the location of the apparent host galaxy NGC 4993 in the Swope optical discovery image at 10.9 hr after the merger (top right) and the DLT40 pre-discovery image from 20.5 days prior to merger (bottom right). The reticle marks the position of the transient in both images.

EM Observations

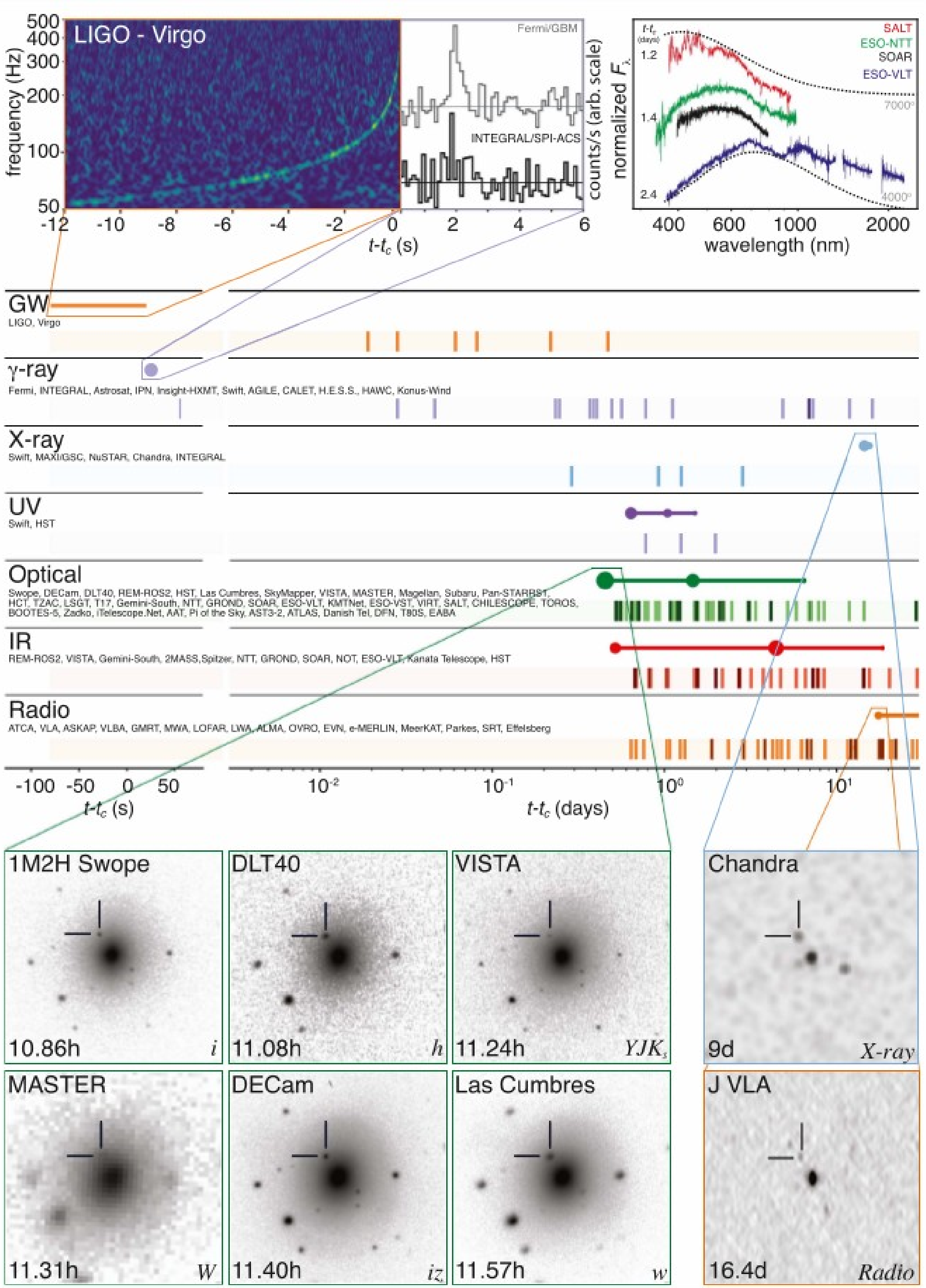

Figure 2. Timeline of the discovery of GW170817, GRB 170817A, SSS17a/AT 2017gfo, and the follow-up observations are shown by messenger and wavelength relative to the time t_c of the gravitational-wave event. Two types of information are shown for each band/messenger. First, the shaded dashes represent the times when information was reported in a GCN Circular. The names of the relevant instruments, facilities, or observing teams are collected at the beginning of the row. Second, representative observations (see Table 1) in each band are shown as solid circles with their areas approximately scaled by brightness; the solid lines indicate when the source was detectable by at least one telescope. Magnification insets give a picture of the first detections in the gravitational-wave, gamma-ray, optical, X-ray, and radio bands. They are respectively illustrated by the combined spectrogram of the signals received by LIGO-Hanford and LIGO-Livingston (see Section 2.1), the *Fermi*-GBM and *INTEGRAL*/SPI-ACS lightcurves matched in time resolution and phase (see Section 2.2), $1\overset{\prime}{.}5 \times 1\overset{\prime}{.}5$ postage stamps extracted from the initial six observations of SSS17a/AT 2017gfo and four early spectra taken with the SALT (at $t_c + 1.2$ days; Buckley et al. 2017; McCully et al. 2017b), ESO-NTT (at $t_c + 1.4$ days; Smartt et al. 2017), the SOAR 4 m telescope (at $t_c + 1.4$ days; Nicholl et al. 2017d), and ESO-VLT-XShooter (at $t_c + 2.4$ days; Smartt et al. 2017) as described in Section 2.3, and the first X-ray and radio detections of the same source by *Chandra* (see Section 3.3) and JVLA (see Section 3.4). In order to show representative spectral energy distributions, each spectrum is normalized to its maximum and shifted arbitrarily along the linear y-axis (no absolute scale). The high background in the SALT spectrum below 4500 Å prevents the identification of spectral features in this band (for details McCully et al. 2017b).

GW170817 Made lots of Gold

Not only did the observations confirm the theoretical predictions, but the modeling allowed Kasen and his colleagues to calculate the amount and chemical makeup of the material produced. The scientists inferred that around 6 percent of a solar mass of heavy elements were made. The yield of gold alone was around 200 Earth masses, and that of platinum nearly 500 Earth masses.

Read more at:
https://phys.org/news/2017-10-astronomers-cosmic-gold-precious-metals.html#jCp

GW170817 Summary

- First Binary Neutron Star merger GW.
- First GW observation with EM confirmation.
- Strongest GW yet, closest.
- Fifth direct detection of GWs by LIGO.
- Independent observation of a “modest” Gamma Ray Burst seems to confirm they come form BNS mergers.
- About half of all heavy elements come from Supernova (old thinking was all) and about half from BNS mergers.

Backup

- aa

General Relativity

- Albert Einstein’s theory of Gravity, generally called his General Theory of Relativity, published in 1915-16.
- Followed his Special Theory of Relativity in 1905 which describes connecting the physics between to observers moving with a uniform velocity relative to each other. These are usually called “inertial frames.”

GR makes predictions for more extreme objects.

- Compact objects, especially neutron stars (pulsars) and black holes have very strong gravitational fields.
- Binary stars / black holes /neutron stars will emit gravitational radiation and lose orbital energy.
  - Note the good fit to the Hulse-Taylor pulsar PSR J1915+1606 (and other names too). Considered first evidence for GWs.
  - LIGO announced first direct detection of GWs in February 2017 about an even the previous September 2015: GW150914 .

GR passes all “weak field” tests.

- GR passes all the tests for it that we can devise in our part of the universe.
  - The anomalous precession of the perihelion of Mercury’s orbit. Most due to the large planets perturbing the orbit and the oblate sun, 450 arc-seconds per century, but measure 490. GR predicts the missing 40 because of the effective gravitational well for the planet.
  - Our star bends light---Eddington 1919 (check?). Now routinely used to study matter distributions (gravitational lensing) and single stars or rogue planets (micro-lensing).
  - Clocks run slower lower in a gravitational well---atomic clocks on airplanes (xxx), frequency of light from atoms deep in a start, GPS satellite clocks.

Black Hole Binary Coalescence Emits GWs.

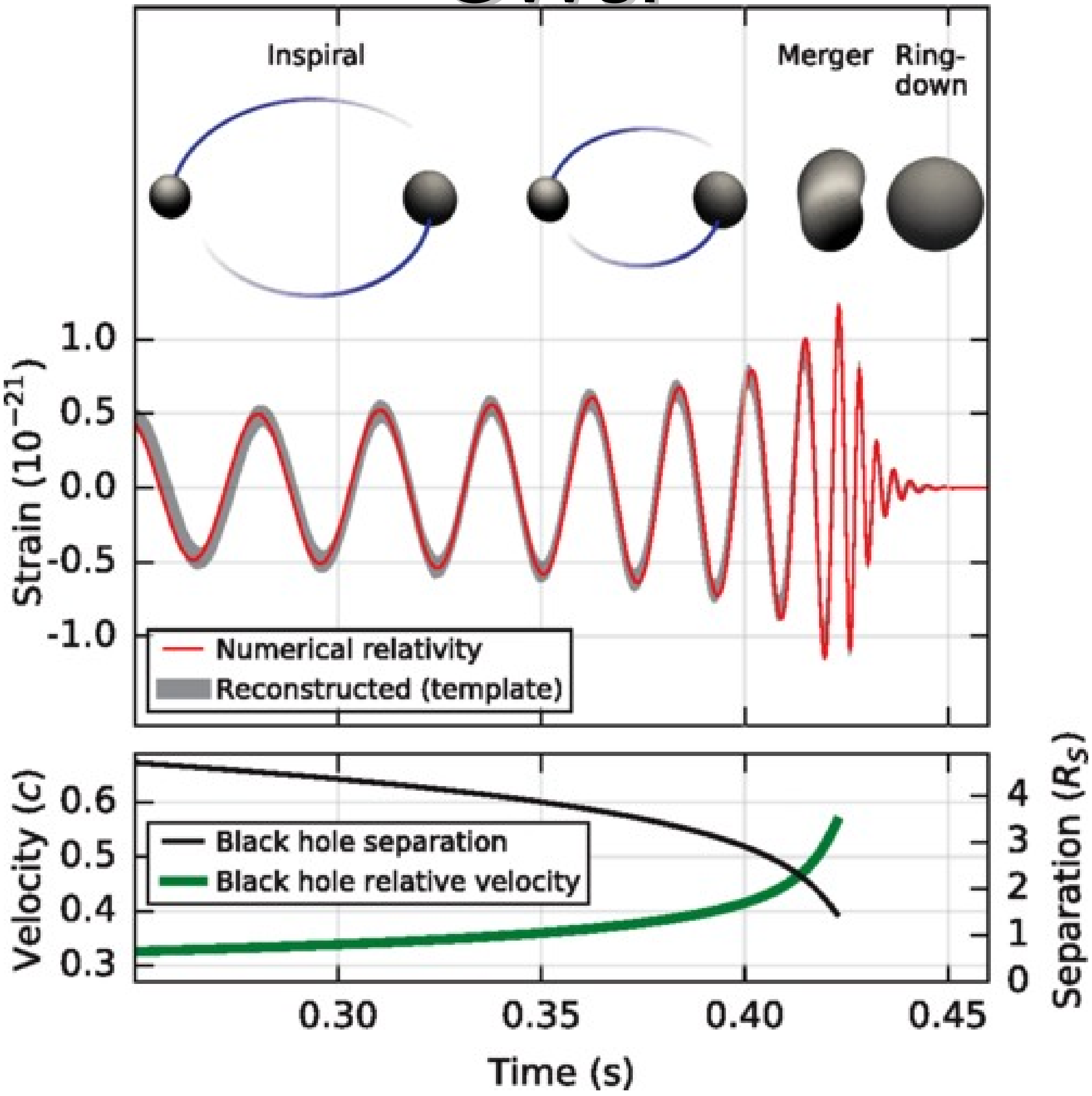

Strain Curves from Moore et al.

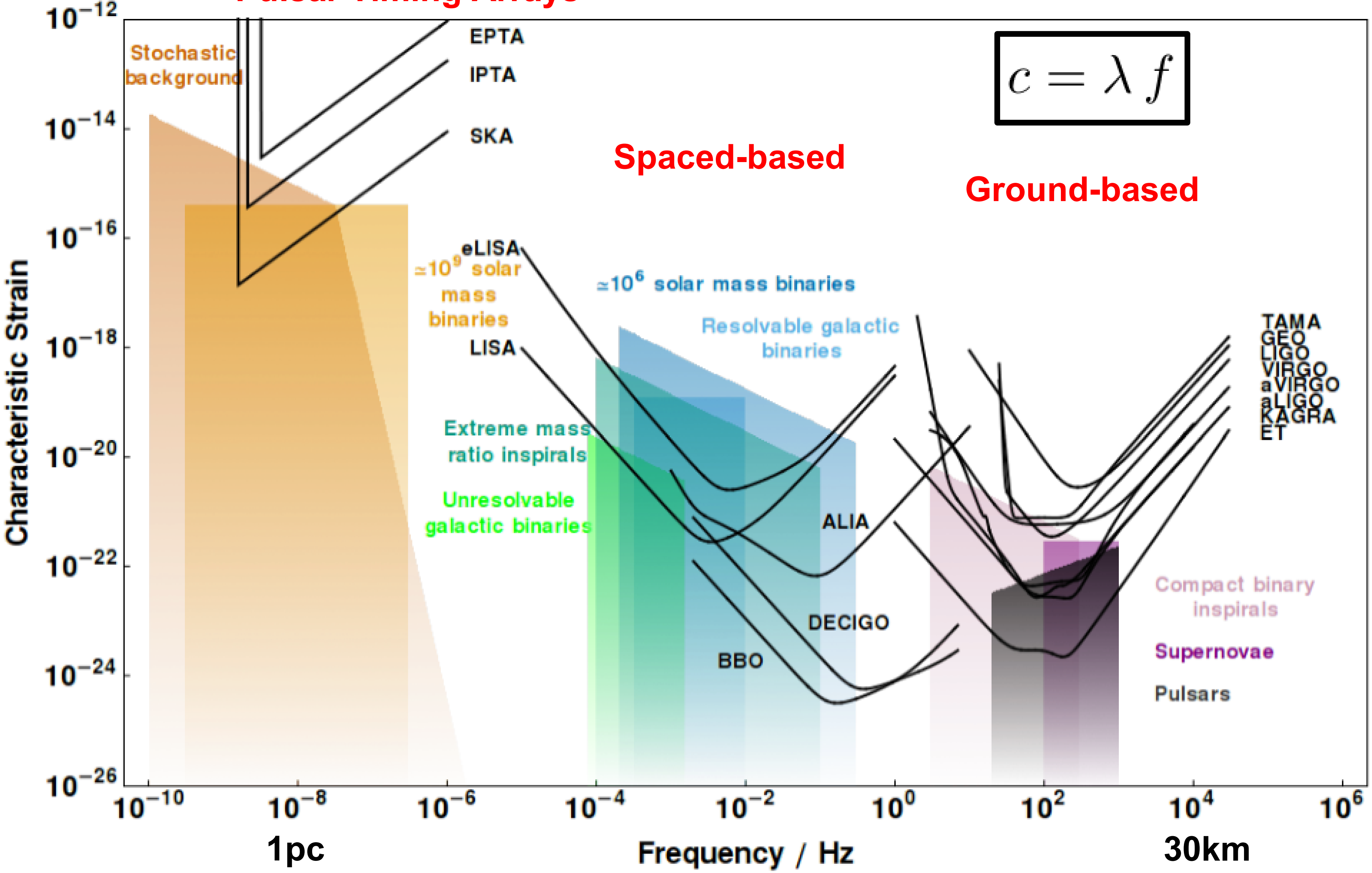

Pulsar Timing Arrays

Spaced-based

Ground-based

$$c = \lambda f$$

1pc **30km**

wavelength, m **3e16** **3e12** **3e8** **3e4**

)

Gravitational Wave Spectrum

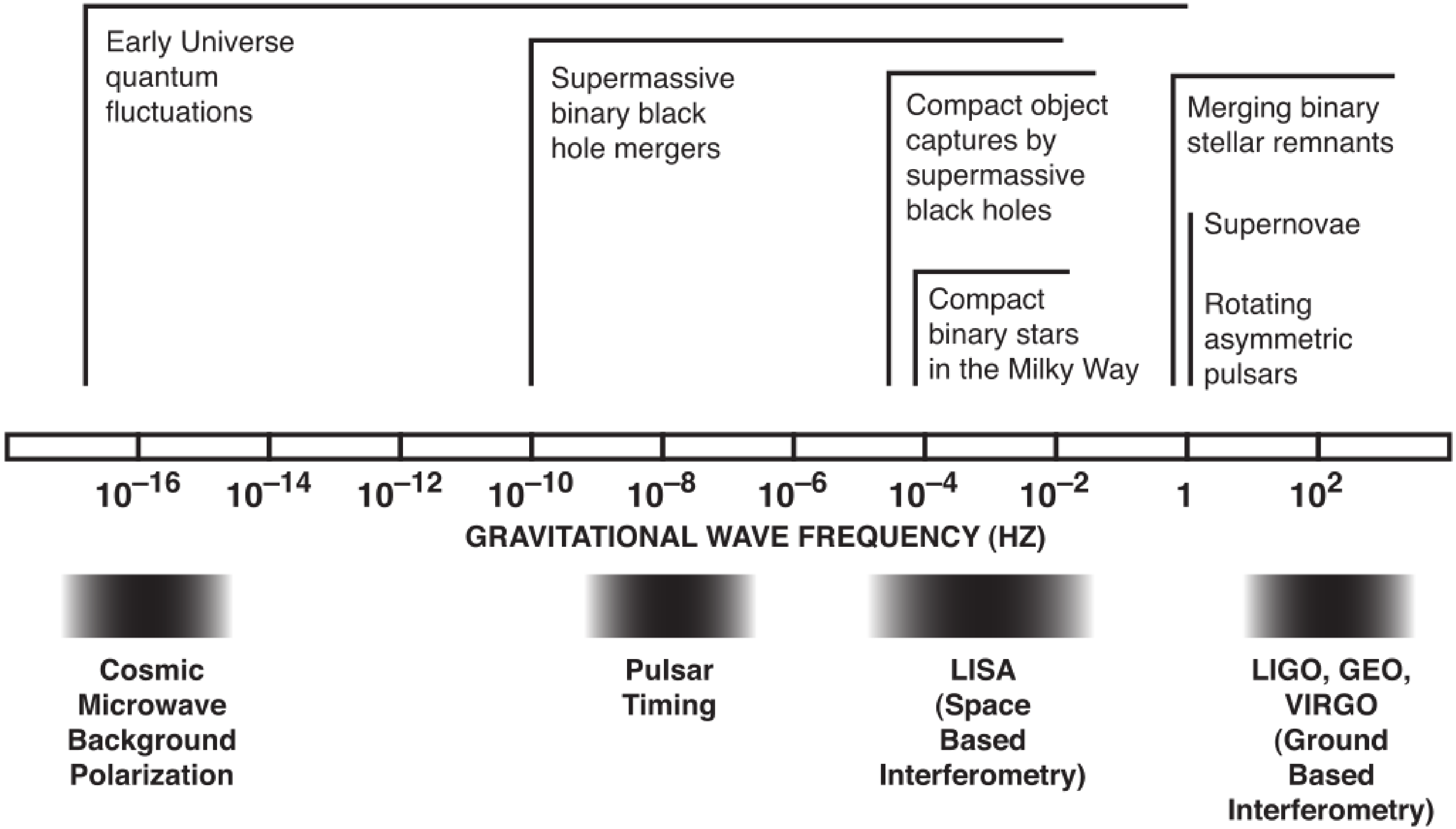

Early Universe quantum fluctuations

Supermassive binary black hole mergers

Compact object captures by supermassive black holes

Compact binary stars in the Milky Way

Merging binary stellar remnants

Supernovae

Rotating asymmetric pulsars

10^{-16} 10^{-14} 10^{-12} 10^{-10} 10^{-8} 10^{-6} 10^{-4} 10^{-2} 1 10^{2}

GRAVITATIONAL WAVE FREQUENCY (HZ)

Cosmic Microwave Background Polarization

Pulsar Timing

LISA (Space Based Interferometry)

LIGO, GEO, VIRGO (Ground Based Interferometry)

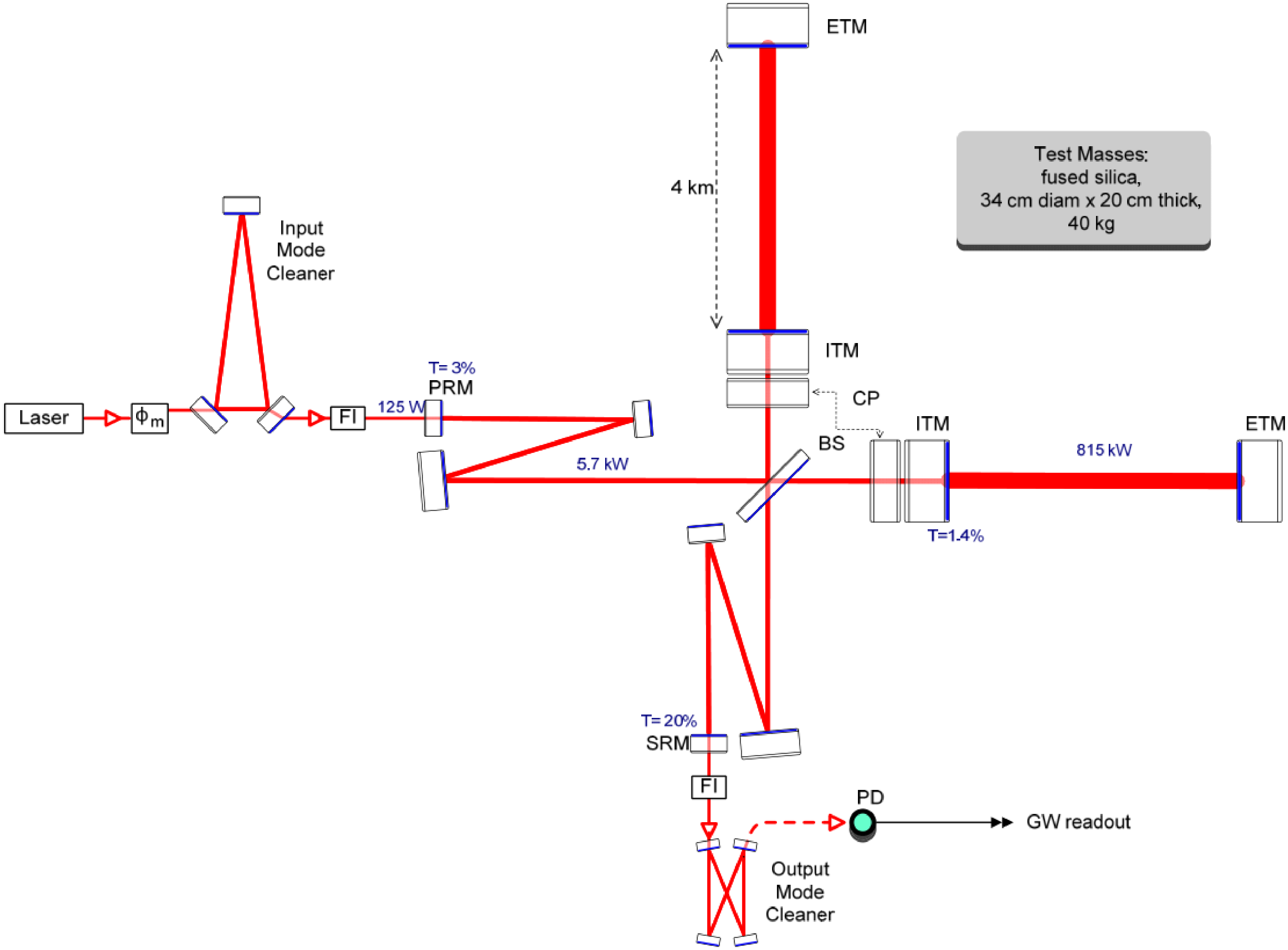

Test Masses:
fused silica,
34 cm diam x 20 cm thick,
40 kg

Nature of Gravitational Waves, and $h_{\mu\nu}$

Of all 10 possible components to h, it simplifies to two polarizations. One with a motion that shrinks (grows) in one direction while growing (shrinking) in the other direction. The other polarization is just rotated by 45 degrees.

h_+

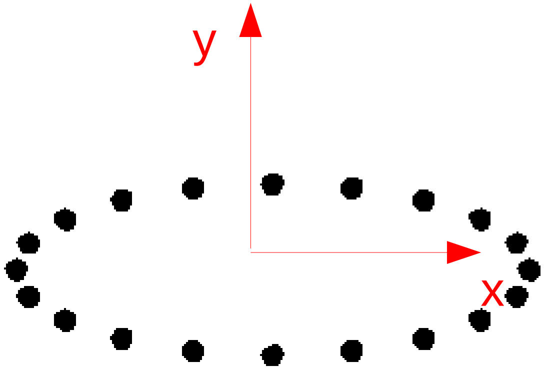

hplus polarization

$h_\times$

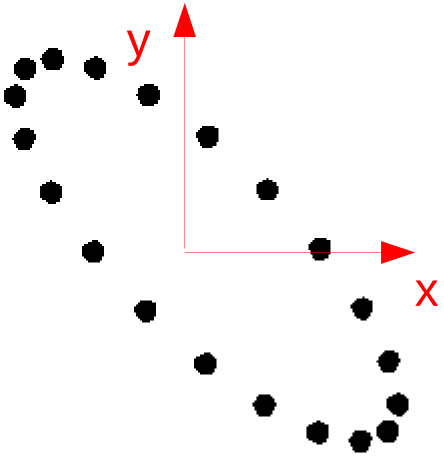

hcross polarization

Wave headed into the page, Y up, X right.

Effect of a perfectly aligned wave on LIGO

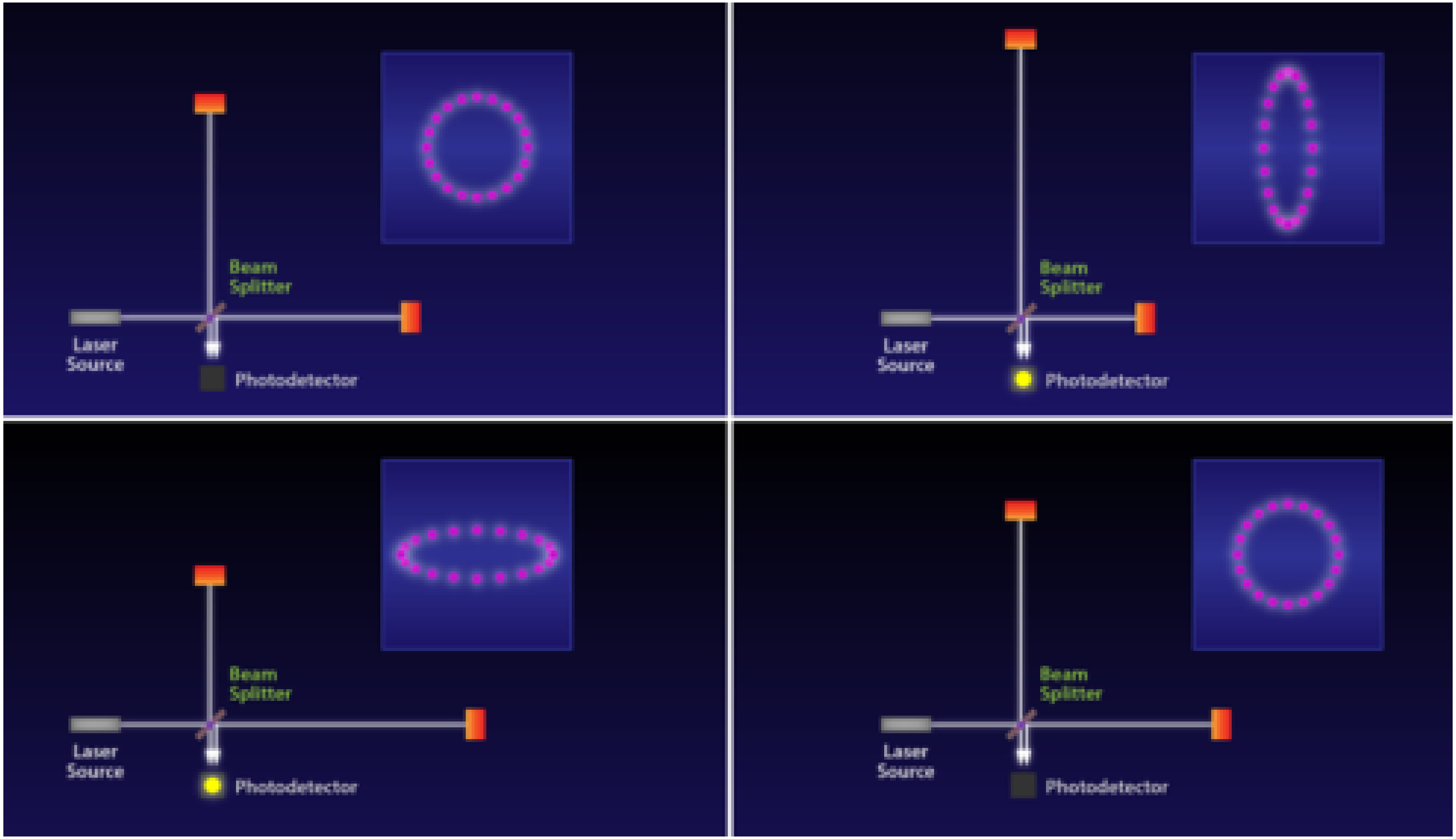

LIGO

LIGO Sites

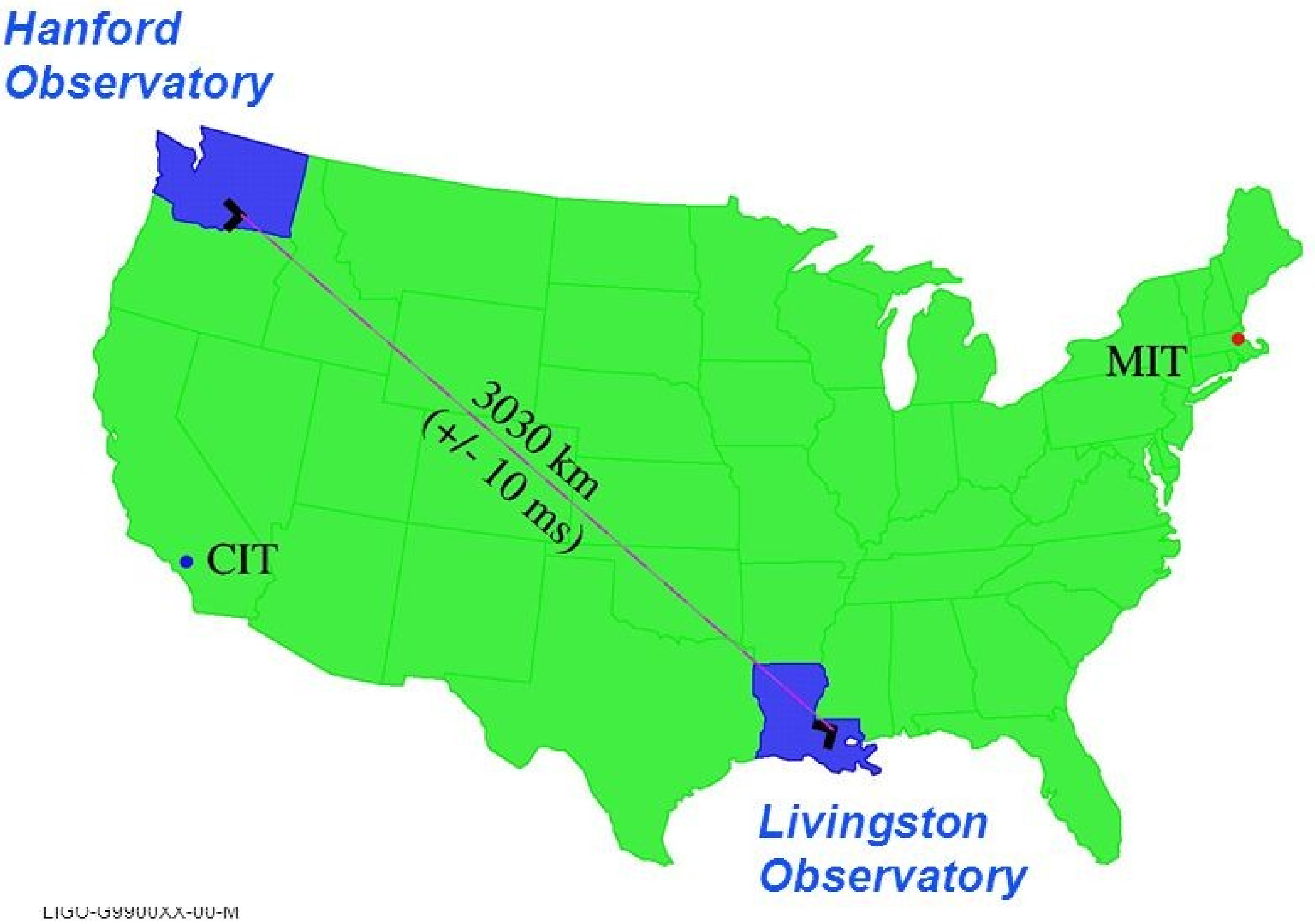

Seismic Noise aLIGO and initial

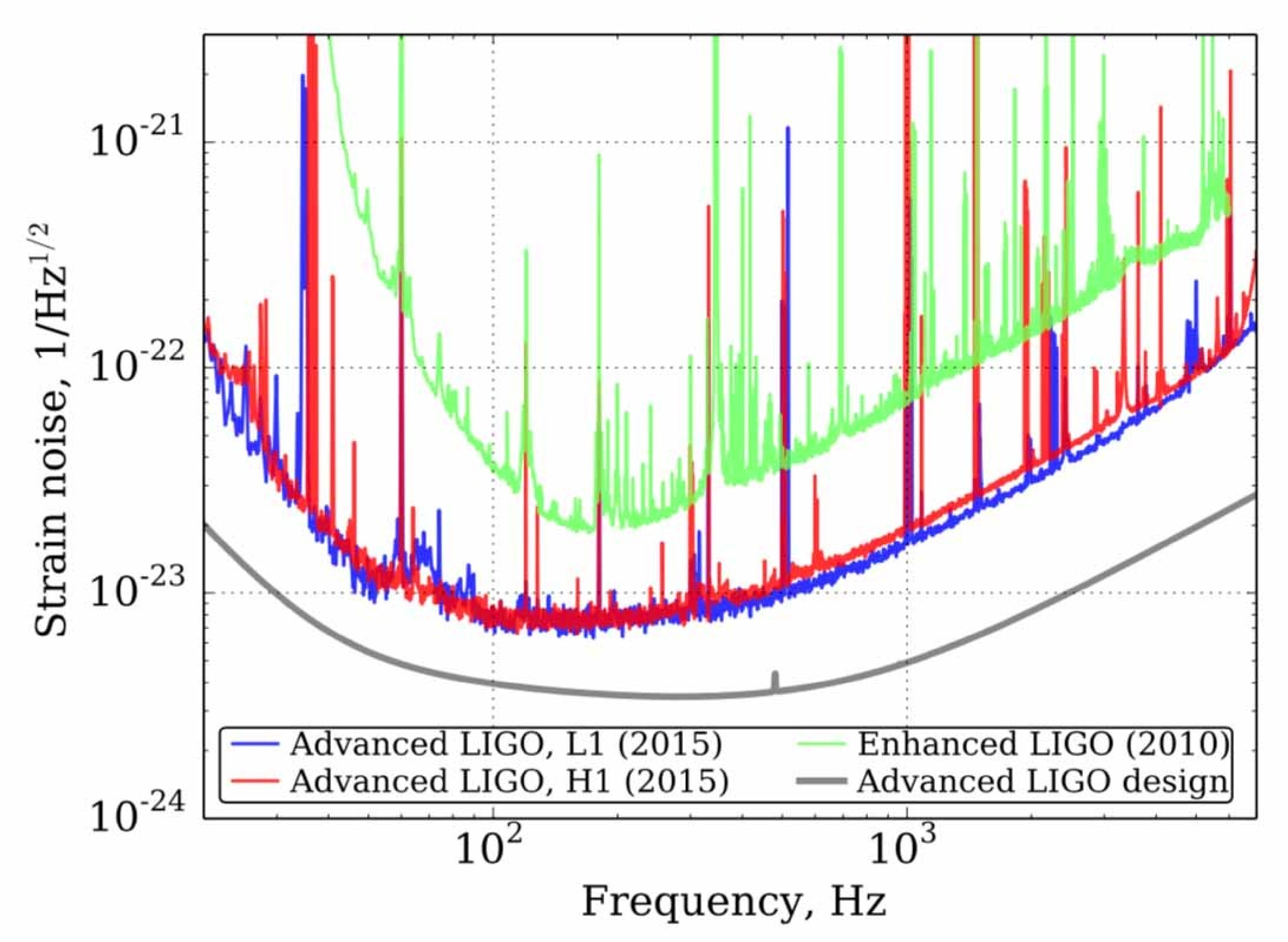

LISA and eLISA

- LISA has a full equilateral triangle of lasers and baseline of 5e9 m. Not funded.

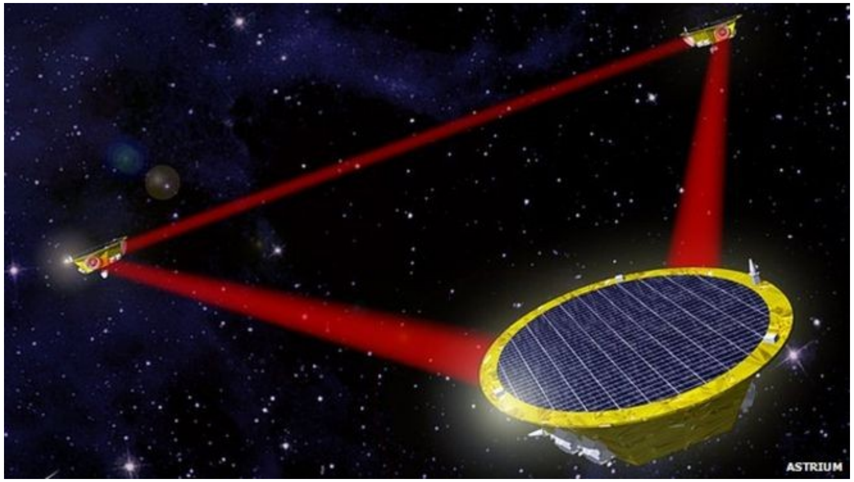

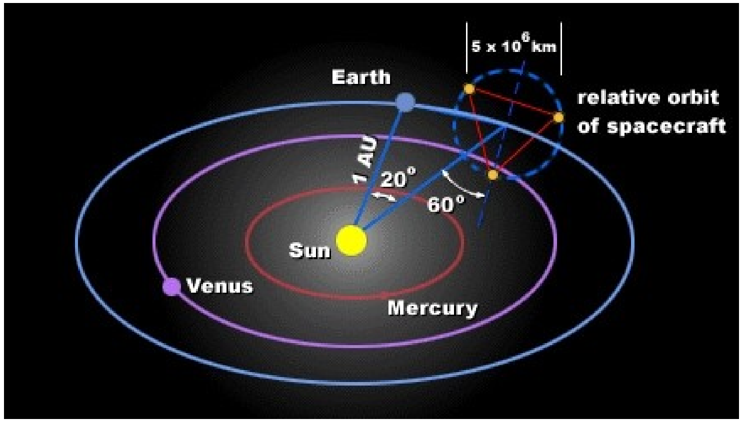

- eLISA uses two legs of the equilateral triangle of lasers and baseline of 1e9 m. Successful LISA Pathfinder mission and LIGO detection means likely to go forward and maybe “fast-tracked.”

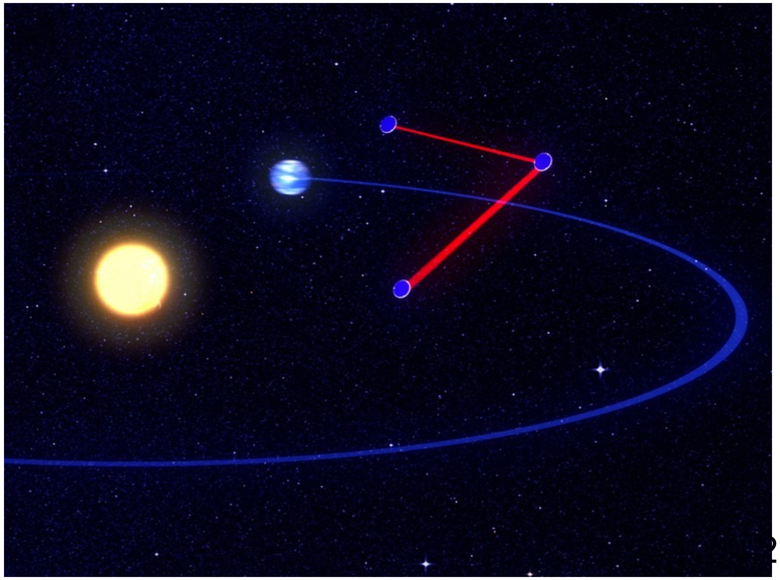

LISA Pathfinder

- LISA Pathfinder successfully demonstrated the technologies for “drag-free” flight of the eLISA space craft.
  - Orbit is *nearly* freely falling around the sun.
  - Microthrusters used to counter solar wind, etc, and allow a free mass inside to react only to gravity!

- Measured relative acceleration as good as 6e-15 m/s^2 per root Hz (tomorrow).

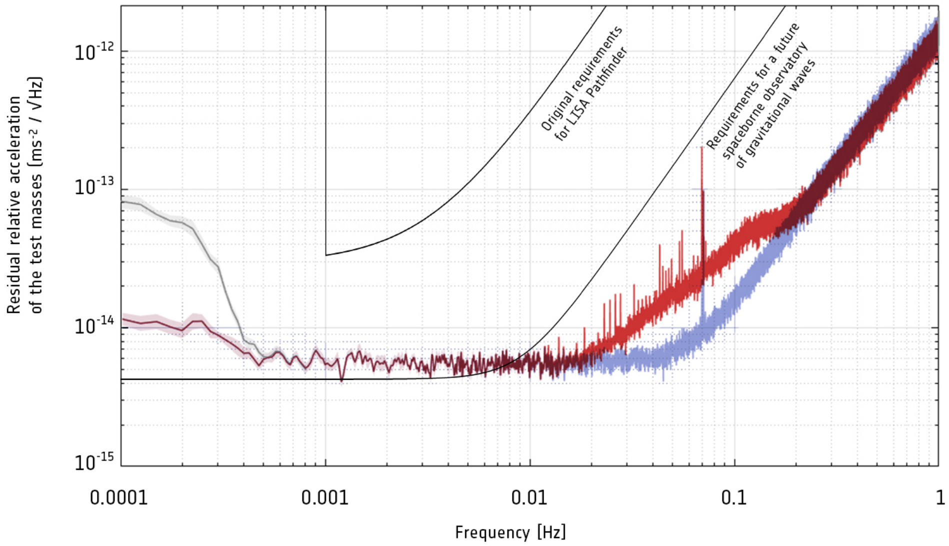

LISA Pathfinder

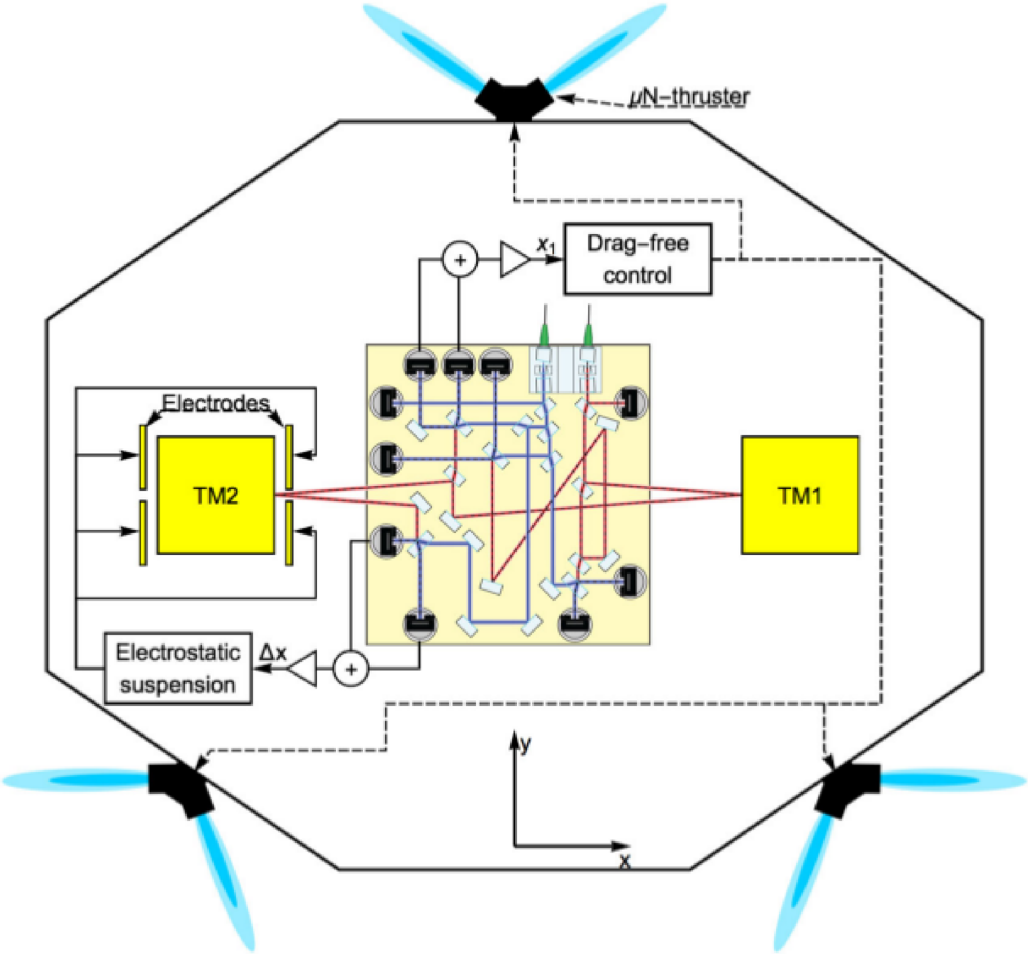

FIG. 2. A schematic of LPF. The figure shows TM1, TM2, and the optical bench beam paths for measuring Δx and x_1. The measurement of Δx drives the electrostatic suspension of TM2, which applies the necessary electrostatic forces by means of the electrodes represented by the four gold plates facing TM2. All other electrodes surrounding the TMs are not shown. The measurement of x_1 drives the drag-free control loop that uses the micronewton thrusters to exert forces on the spacecraft. The figure depicts the x and y axes we use in this Letter, while z is normal to the figure.

Ref: Armano et al., PRL 2016

LISA Pathfinder

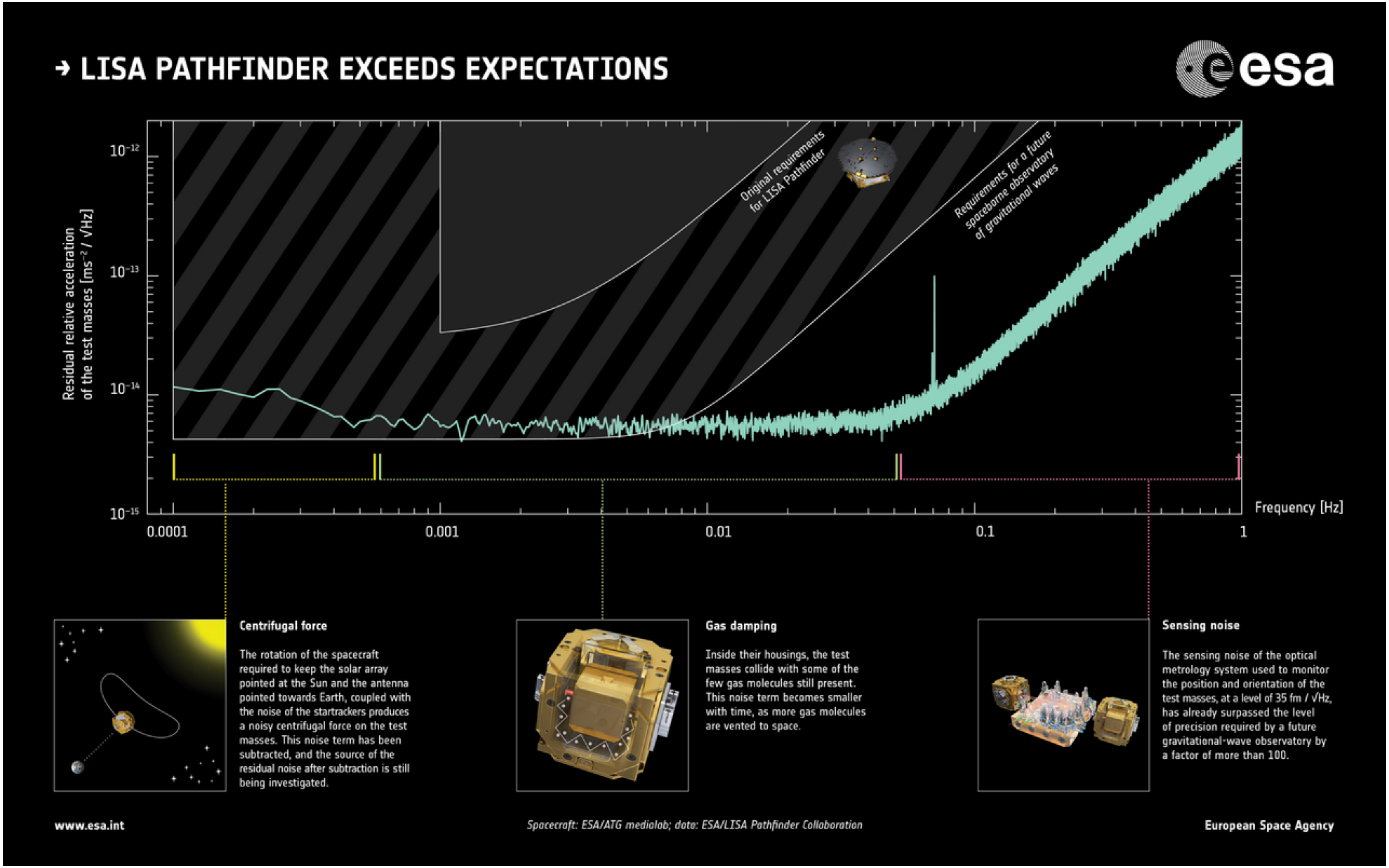

→ LISA PATHFINDER EXCEEDS EXPECTATIONS

Centrifugal force

The rotation of the spacecraft required to keep the solar array pointed at the Sun and the antenna pointed towards Earth, coupled with the noise of the startrackers produces a noisy centrifugal force on the test masses. This noise term has been subtracted, and the source of the residual noise after subtraction is still being investigated.

Gas damping

Inside their housings, the test masses collide with some of the few gas molecules still present. This noise term becomes smaller with time, as more gas molecules are vented to space.

Sensing noise

The sensing noise of the optical metrology system used to monitor the position and orientation of the test masses, at a level of 35 fm / √Hz, has already surpassed the level of precision required by a future gravitational-wave observatory by a factor of more than 100.

www.esa.int

Spacecraft: ESA/ATG medialab; data: ESA/LISA Pathfinder Collaboration

European Space Agency

Pulsar Timing Arrays

- Millisecond pulsars are very good clocks scattered around the Universe.
- By measuring them once in a while, you can detect a hiccup in the reception of the pulse at Earth. With enough "clocks" you can decide if there was a gravitational wave and from where it may have come.
- See chart, sensitive to very, very long wavelengths, and thus very, very small frequencies. Size of the Universe sort of waves!

Ref: NANOGrav collaboration

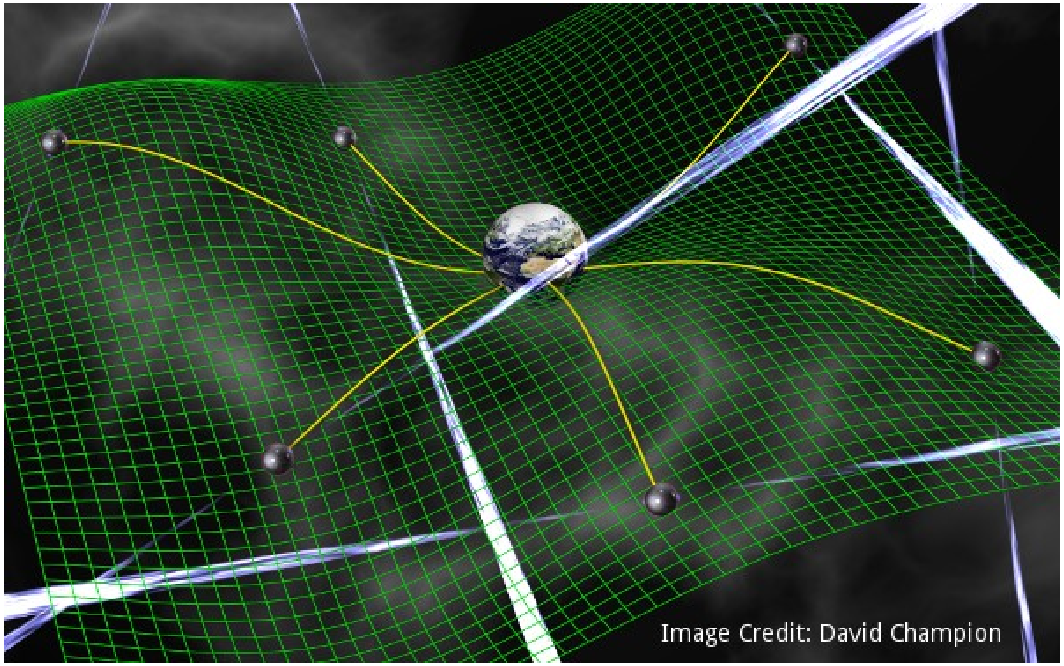

Image Credit: David Champion

Pulsar Timing Arrays

- Several collaborations working at radio astronomy facilities to measure millisecond pulsars:
- NANOGrav, US and NASA, using Arecibo and Green Bank.
- The International Pulsar Timing Array uses many radio telescopes.
- The European Pulsar Timing Array
- and others.

Links

- CalTech GW media assets page.
- Kelly Holley-Bockelman's TEDx Nashville Talk 2016 about GW150914.
- Pulsar timing array, Nanograv

Some Constants

Schwarzschild radius	2GM/c^2	2953 m for Msun
GR Units, Mass	GM/c^2	1477 m for Msun
GR Units, Power	c^5/G	3.628e52 W
GR Units, Energy	c^4/G	1.210e44 J/m
parsec, pc		3.09e16 m = 3.262 ly
astronomical unit, au		149.6e9 m
light-year, ly		0.946e16 m = 0.307 pc
fine structure constant	e^2/(4pi eps0)/hbar c	0.00730 = 1/137.04
wavelength-energy	h c	1.24 eV μm